Variation of passivation behavior induced by sputtered energetic particles and thermal annealing for ITO/SiO_x/Si system*

Ming Gao(高明)[1], Hui-Wei Du(杜汇伟)[1], Jie Yang(杨洁)[1], Lei Zhao(赵磊)[1], Jing Xu(徐静)[2], and Zhong-Quan Ma(马忠权)[1,2,†]

[1] *SHU-SOEN's Research and Development Laboratory, Department of Physics, Shanghai University, Shanghai* 200444, *China*
[2] *Instrumental Analysis and Research Center, Shanghai University, Shanghai* 200444, *China*

(Received 22 November 2016; revised manuscript received 18 January 2017; published online 20 February 2017)

The damage on the atomic bonding and electronic state in a SiO_x(1.4–2.3 nm)/c-Si(150 μm) interface has been investigated. This occurred in the process of depositing indium tin oxide (ITO) film onto the silicon substrate by magnetron sputtering. We observe that this damage is caused by energetic particles produced in the plasma (atoms, ions, and UV light). The passivation quality and the variation on interface states of the SiO_x/c-Si system were mainly studied by using effective minority carrier lifetime (τ_{eff}) measurement as a potential evaluation. The results showed that the samples' τ_{eff} was reduced by more than 90% after ITO formation, declined from 107 μs to 5 μs. Following vacuum annealing at 200 °C, the τ_{eff} can be restored to 30 μs. The components of Si to O bonding states at the SiO_x/c-Si interface were analyzed by x-ray photoelectron spectroscopy (XPS) coupled with depth profiling. The amorphous phase of the SiO_x layer and the "atomistic interleaving structure" at the SiO_x/c-Si interface was observed by a transmission electron microscope (TEM). The chemical configuration of the Si–O fraction within the intermediate region is the main reason for inducing the variation of Si dangling bonds (or interface states) and effective minority carrier lifetime. After an appropriate annealing, the reduction of the Si dangling bonds between SiO_x and near the c-Si surface is helpful to improve the passivation effect.

Keywords: sputtered damage, SiO_x/c-Si interface, effective minority carrier lifetime, XPS

PACS: 52.20.Hv, 68.35.–p, 68.37.–d, 73.20.–r **DOI:** 10.1088/1674-1056/26/4/045201

1. Introduction

Indium tin oxide (ITO) film has been widely used as transparent conductive oxide (TCO) in the efficient silicon-based heterojunction solar cells, owing to its "semiconductor-assisted role"[1] and "window function".[2] Usually, the ITO film has been made by the sol–gel method,[3] chemical vapor deposition,[4] magnetron sputtering,[5] and so on. The radio frequency (RF) magnetron sputtering is the most common method to deposit ITO film on a substrate because of its advantages in reproducibility, uniformity and film properties.[2,5,6] However, during the ITO deposition process, the energetic particle beam in the plasma will cause damage on the atomic bonding and electronic state of the substrate.[6–12] For ITO/SiO_x/n-Si (SIS) devices, if the SiO_x is formed prior to ITO film, the sputtering would damage the electronic structure of the SiO_x layer and SiO_x/c-Si interface, increasing the interface recombination rate and decreasing the diffusion length of carriers, and leading to a loss in the open circuit voltage and the short circuit current of the device, respectively. This negatively affects the power conversion efficiency of the device. The researchers usually focus on the passivation effect before sputtering of ITO or the overall performance of those kinds of devices, and ignore sputtering damage in the efficient silicon-based heterojunction solar cells, especially for the HIT (Heterojunction Intrinsic Thin Films) and SIS (Semiconductor-Insulator-Semiconductor) device.

In this report, three techniques have been applied for the evaluation of the intermediate region modified by energetic beams during ITO sputtering. Firstly, effective minority carrier lifetime (τ_{eff}) is a physical parameter to assess the interface recombination rate caused by sputtering degradation. The τ_{eff} is usually measured by a microwave photoconductivity decay (μ-PCD) method in the solar cell production line, evaluating the surface passivation effect of semiconductor materials.[13,14] Secondly, according to the surface model of silicon oxide reported by Seah *et al.*,[15] typically non-stoichiometric silicon oxides of Si_2O, SiO, and Si_2O_3 exist in the SiO_x/c-Si interface whether formed or induced by other interactions, corresponding to the charged electronic states of Si^{1+}, Si^{2+}, and Si^{3+}, respectively. The fixed positive charges and interface states in the vicinity of SiO_x/c-Si stem from sub-oxide SiO_x, inducing the carriers' recombination and affecting samples' τ_{eff}. Thus, the chemical composition and phase structure of the SiO_x/c-Si interface are critical for the performance of an optoelectronic device and are required to be figured out by powerful characterization methods, such as either x-

*Project supported by the National Natural Science Foundation of China (Grant Nos. 61274067, 60876045, and 61674099) and the Research and Development Foundation of SHU-SOENs PV Joint Laboratory, China (Grant No. SS-E0700601).

†Corresponding author. E-mail: zqma@shu.edu.cn

© 2017 Chinese Physical Society and IOP Publishing Ltd

ray photoelectron spectroscopy (XPS) with depth profiling or transmission electron microscope (TEM) for the microstructure confirmation. In addition, the post-annealing of a semiconductor is an effective method to lessen the interface states and the charge traps of the materials and devices.[16] On the other hand, thermal annealing in a high vacuum chamber can avoid impurity contaminants. Therefore, we first measured the τ_{eff} of the samples with different treatments using μ-PCD, and studied the origin of the sputtered damage at the SiO_x/c-Si interface. Afterwards, we investigated the variation of τ_{eff} under the variable temperature annealing conditions, and discussed the electronic structures and chemical bonding of SiO_x/c-Si in the interfacial region corresponding to the different samples with a specific τ_{eff}.

2. Experimental in details

2.1. Preparation of samples

Solar grade n-type Czochralski silicon [(100), phosphor doped, chemical polished, (1.5–3.0) Ω·cm, (150±3) μm, 3.0 cm×3.0 cm] was cleaned by a standard RCA method.[17] Silicon wafers were first dipped into 0.08-mol/L iodine, which is considered as the best passivation to silicon.[13,14] Passivated samples were sequentially sonicated for 10 min in absolute ethanol, deionized water, removing iodine. An ultrathin (∼ 2 nm) SiO_x layer was formed by thermally oxidizing in an oxidation furnace for 10 min at 700 °C. The flow ratio of high purity nitrogen and oxygen was 4 L/min: 1 L/min. It was verified that the thin SiO_x layer was involved into four compositions: lots of SiO_2, very few of Si_2O, SiO, and Si_2O_3 (Si 2p peak in the XPS spectrum as shown in Fig. S1 in Appendix A). Subsequently, ITO films of about (80±3) nm were deposited by the radio frequency magnetron sputtering system. The ITO target used for sputtering purposes was a sintered ceramic mixture disk of 10-wt% SnO_2 and 90-wt% In_2O_3. The base pressure was 3×10^{-4} Pa for the sputtering system. The substrate temperature of 250 °C, a power of 100 W, an argon partial pressure of 1.0 Pa and an argon gas flow rate of 40 sccm were set during the ITO film deposition, respectively. The carrier concentration, electronic mobility, and resistivity of ITO film were $(3.79 \pm 0.04) \times 10^{20}$ cm^{-3}, (39.4 ± 0.8) $cm^2 \cdot V^{-1} \cdot S^{-1}$, $(4.18 \pm 0.07) \times 10^{-4}$ Ω·cm, respectively, which were measured by Hall Effect measurement. The average transmittance of visible spectrum was more than 85% and the optical band gap was deduced to be 3.60 eV (as shown in Fig. S2 in Appendix A), which was measured by a UV-VIS spectrophotometer.

To compare the passivation effectiveness, sputtering damage and annealing effect, the samples were divided into two groups. (i) The first set of samples, which were successively cleaned by immersion in 37% concentrated hydrochloric acid, deionized water and 5% hydrofluoric acid, removing both the ITO film and the silicon oxide layer. Then, samples are secondary passivated by 0.08-mol/L iodine. For the comparison, ITO films were directly deposited on two-sides of the unoxidized silicon substrate, with the same process of magnetron sputtering and treatment conditions. (ii) The second set of samples, which were annealed at the temperatures of 100 °C–700 °C (step length of 100 °C) for 30 min in the transfer sample chamber of the magnetron sputtering apparatus. The working pressure was maintained at 1×10^{-3} Pa. By contrast, ITO films are directly deposited on two-sides of seven unoxidized silicon wafers, with the same process of magnetron sputtering and post-annealing.

2.2. Characterization

The τ_{eff} was measured using a μ-PCD instrument (Semilab WCT-2000) with two-dimensional image. A 200-ns laser pulsed at 904 nm was used for the gain of photon-generated carriers. The number of photons in one pulse was 1.20×10^{19}. Each sample was scanned three times at 1 mm×1 mm resolution. Silicon wafer treated with iodine was encapsulated in a plastic bag to prevent contamination prior to be contacted by the prober. The electronic states and the chemical bonding of ITO/SiO_x/c-Si samples were examined by XPS with depth profiling (Thermo Fisher Scientific ESCA-250Xi). The sample was etched by Ar^+ ion beam with 1 keV, and the etching step was 20 s. A monochromatic Al Kα excitation source ∼ 1486.60 eV was used for the XPS measurements. The pass energy of 30.00 eV, scan step of 0.10 eV and test area of 500 μm×500 μm were set for testing. The lattice array morphology of ITO film, SiO_x layer and SiO_x/c-Si interface were analyzed by a TEM (JEOL JEM-2010 F) operated at 200 kV.

In the τ_{eff} measurements, an *x*–*y* two-dimensional coordinate system was taken for the fixed-points to monitor the changes of τ_{eff} before and after depositing ITO film or annealing, so that the lateral non-uniformity of the sample could be avoided. The measuring principle was designed as: at the fixed-point beside the central region, each of τ_{eff} was adopted to the average value, and the consistency of seven measurements in τ_{eff} before and after sputtering of ITO film was guaranteed. The average value of τ_{eff} was taken from three-time measurements and a standard deviation was derived.

3. Results and discussion

3.1. Effect of sputtering ITO on effective minority carrier lifetime

Generally, for the high pure silicon wafer, the minority carrier lifetime (τ_{eff}) is substantially determined by both the

bulk minority carrier lifetime ($\tau_{\rm bulk}$) and the surface minority carrier lifetime ($\tau_{\rm surf}$) as shown in the following equation[13,18]

$$\begin{cases} \dfrac{1}{\tau_{\rm eff}} = \dfrac{1}{\tau_{\rm bulk}} + \dfrac{1}{(\tau_{\rm diff} + \tau_{\rm surf})}, \\ \tau_{\rm diff} = \dfrac{d^2}{(\pi^2 \times D_{n,p})}, \\ \tau_{\rm surf} = \dfrac{d}{(2 \times S)}, \end{cases} \tag{1}$$

where $\tau_{\rm diff}$ is the diffusion time for minority carriers from the interior of the wafer to the surface, decided by the wafer thickness (d) and the diffusion coefficient of minority carriers ($D_{\rm n,p}$); $\tau_{\rm surf}$ is determined by wafer thickness (d) and surface recombination velocity (S). When the silicon surface is passivated by 0.08-mol/L iodine which is considered as the best passivation to silicon, S is very low, and the $\tau_{\rm eff}$ primarily indicates the bulk characteristics of the wafer. When the silicon surface is not passivated, S is very high, so the $\tau_{\rm eff}$ will be dominant by the surface feature of the wafer.[13,14]

Figure 1 shows the variation of minority carrier lifetime 2D distribution of the one silicon wafer under the different states. As shown in Figs. 1(b) and (c), for those passivated samples undergoing furnace oxidation, the ITO sputtering process leads to a loss in $\tau_{\rm eff}$ of over 90%, dropping to about 5 μs. For the collected data in Figs. 1(a), 1(d), and 1(f), the $\tau_{\rm eff}$ is basically maintained steady when it is once, twice and thrice passivated by 0.08-mol/L iodine, and S is very low, indicating that the $\tau_{\rm bulk}$ remains unchanged before and after sputtering, and it is larger than 280 μs. By contrast, the surface passivation validity of the sample where the ITO film is directly deposited on two-sides of unoxidized silicon is also poor as shown in Fig. 1(e). As a result, the structural damage should be localized at the SiO_x/c-Si interface, most likely in the form of the deep defects and the Si dangling bonds (or interface states).[19,20]

In order to make clear what the new electronic states are within the intermediate region of ITO/c-Si, after sputtering deposition of ITO thin film, the chemical components in the region are determined by XPS in elemental inner core–electron peaks such as In 3d, Sn 3d, Si 2p, and O 1s, with depth profiling. The relative atomic percent of In, Sn, and Si across the interface of the sample (here ITO film is deposited on silicon after 700-°C/10-min thermal oxidation process) is shown in Fig. 2(a) by an area integral estimation. The depth distribution of the chemical components is divided into three parts with etching times: the front ITO film, the intermediate SiO_x layer, and Si substrate subsequently. At the etching time of 720 s, the measured Si 2p spectra as shown in Fig. 2(c) is dashed dots, while the Si $2p_{3/2}$, Si $2p_{1/2}$, SiO_x, and SiO_2 are the deconvolution, fitted by the likely Si-correlated compositions in the region. According to the surface model of silicon oxide proposed by Seah *et al.*,[15] the Si dangling bond (or interface state) within the SiO_x and SiO_x/c-Si interface is induced by sub-oxide SiO_x, which increases interface recombination and decreases samples' $\tau_{\rm eff}$. However, for the samples without furnace oxidation in advance, just the ITO film being directly deposited on two-sides of silicon substrate, the relative atomic percent of In, Sn, and Si across the interface are given in Fig. 2(b). The depth distribution of chemical components is similar to the former case except a right shift of 40 s. The sub-oxide SiO_x is also observed in Fig. 2(d), corresponding to the SiO_x/c-Si interface. The different finding is that the existence of a broad SiO_x layer at the interface region between ITO and c-Si is also revealed by XPS signal, and SiO_x just come into being in the process of sputtering deposition of ITO film.[21] On the other side, it is reasonable for the right shift of the middle position of the interface region taking place in Fig. 2(b) and a little decrease of the intensity of Si2p peaks in Fig. 2(d), because of the different processing for the two kinds of samples. Therefore, the Si dangling bond appeared in both kinds of samples is identically linked to the sputtering process.

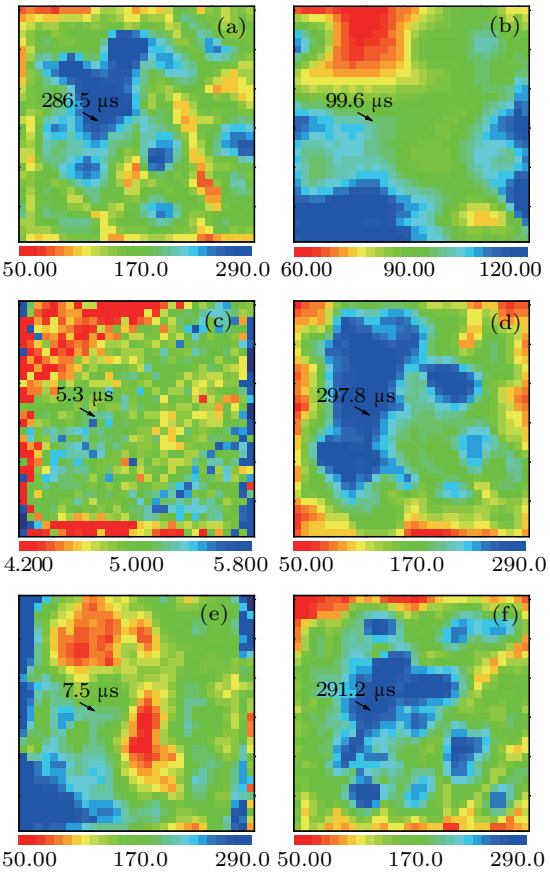


Fig. 1. (color online) Minority carrier lifetime profiles of the identical silicon wafer under the different conditions: (a) a bare silicon is passivated by 0.08-mol/L iodine; (b) 700-°C/10-min thermal oxide passivation; (c) after magnetron sputtering deposition of ITO film; (d) second passivation with 0.08-mol/L iodine; (e) double-sided deposition of ITO film by sputtering on a non-oxidized silicon wafer; (f) third passivation with 0.08-mol/L iodine (unit: μs).

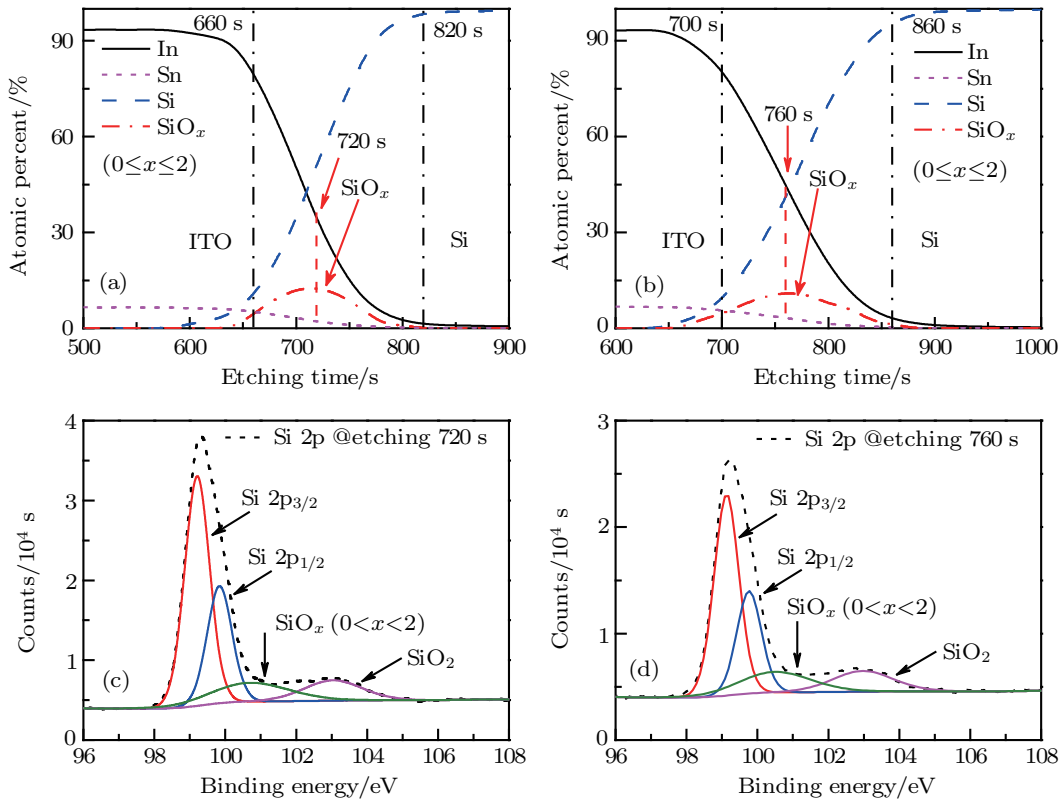


Fig. 2. (color online) The XPS depth profiling of ITO/SiO_x/n-Si structure. (a) ITO film is deposited on silicon after 700 °C/10 min thermal oxidation treatment, relative atomic percent distribution of In, Sn, Si, and SiO_x as a function of etching time; (b) ITO film is directly deposited on two-sides of unoxidized silicon, relative atomic percent distribution of In, Sn, Si, and SiO_x as a function of etching time; (c) Si 2p spectra of etching time at 720 s corresponds to Fig. 2(a); (d) Si 2p spectra of etching time at 760 s corresponds to Fig. 2(b).

Figures 3(a) and 3(b) show the cross-section TEM images of the sample, corresponding to Figs. 2(a) and 2(b), respectively. It is apparent that an ultrathin SiO_x layer presents between the ITO layer and Si substrates in all samples. The thicknesses of SiO_x layers in Figs. 3(a) and 3(b) are separately found to be about 2.3 nm and 1.4 nm. Furthermore, we observed the amorphous phase of the SiO_x layer and "atomistic interleaving structure" at the SiO_x/c-Si interface, which may relate to the intermediate oxidation state of SiO_x and most of the Si dangling bonds.

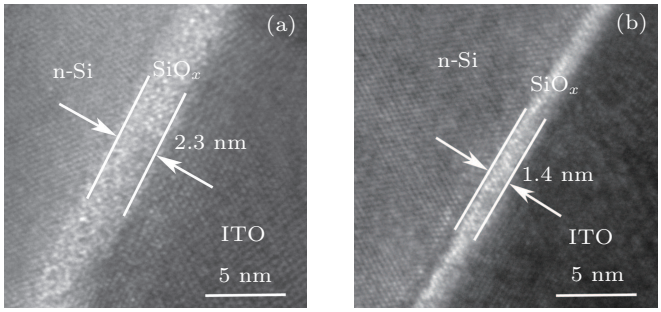


Fig. 3. Cross-sectional TEM micrograph of ITO/SiO_x/n-Si structure. (a) ITO film is deposited on silicon after 700-°C/10-min thermal oxidation treatment; (b) ITO film is directly deposited on two-sides of unoxidized silicon.

We now turn to the origin of the sputtering damage. During the sputtering deposition of ITO film, the average kinetic energy of energetic particles (ions, atoms, molecules, and atomic clusters) is about 10 eV.[22] Oxygen atoms (O^{+0}), oxygen ions ($O^{-1,-2}$), indium atom (In^{+0}), indium ions (In^{+3}), tin atoms (Sn^{+0}), tin ion ($Sn^{+2,+4}$), and reflected argon atoms (Ar^{+0}), argon ions ($Ar^{+1,+2}$) (energies up to 150 eV) primarily bombarded the substrate in the processing of magnetron sputtering.[6,9] The bond energies of Si–Si, Si(Si)–Si, $Si(Si)_2$–Si, Si–O, and Si(O)–O are 3.21, 4.19, 4.56, 8.29, and 4.71 eV, respectively, which are less than that of energetic particles.[23] Therefore, the energetic particles will break the above-mentioned atomic bonds and alter the electron state of the SiO_x layer as well as the SiO_x/c-Si interface, increasing the Si dangling bonds and the interface recombination velocity, and reducing the τ_{eff}. In addition, ultraviolet (UV) radiation from glow discharge and particle collision, reach up to 7.8 eV (or higher), which can pass through the SiO_x layer, reaching to the SiO_x/c-Si interface and the interior of c-Si.[6] UV photons can excite electrons, injecting from the conduction band of Si into the conduction band of SiO_2, activating the deep defects at the SiO_x/c-Si interface and generating additional interface states (or Si dangling bonds). The required energy for this effect is only 3.1 eV, which is less than the UV light energy.[24] Therefore, UV irradiation can damage the SiO_x/c-Si interface, resulting in the attenuation of τ_{eff}. In summary, the Si dangling bonds induced by sputtering damage are consistent with

above experiment results. The Si dangling bonds are created from particle bombardment and UV light irradiation.

3.2. Effect of vacuum annealing on effective minority carrier lifetime

Figure 4 shows the variation of τ_{eff} dependent on the vacuum annealing temperatures, thermal oxidation passivation, and sputtering deposition of ITO on the polished silicon wafer. It is found that a large decrease of τ_{eff} for the samples after a sputtering deposition of ITO films occurs, which means a deterioration of the normally thermal oxidation passivation. The τ_{eff} of c-Si after thermal oxidation at 700 °C for 10 min is constantly kept at 107 μs, while the τ_{eff} is decreased to 5 μs upon subsequent sputtering deposition of ITO films. The likely interpretation is the worsening of the saturation of surface dangling bonds on c-Si, as the τ_{bulk} may not be changed during the sputtering deposition of ITO films. However, the damage of SiO_x/c-Si interface states is partially repaired after vacuum annealing under 100 °C–400 °C for 30 min, improving the τ_{eff} of the samples. The τ_{eff} increases at first and then decreases with the temperature. Herein the τ_{eff} is recovered to nearly 30 μs at 200 °C for 30 min, after that it is declined with the temperature until to about 3 μs after 500 °C. These changes of the τ_{eff} can be verified by a two-dimensional mapping measurement as shown in Fig. 5. Figures 5(a), 5(b), and 5(c) are corresponding to the thermal oxidation, sputtering deposition of ITO, and vacuum annealing at 200 °C, respectively. It should be mentioned that all measurements of the τ_{eff} for the different situation are taken at those fixed points according to the former established x–y frame of axes on the c-Si wafer.

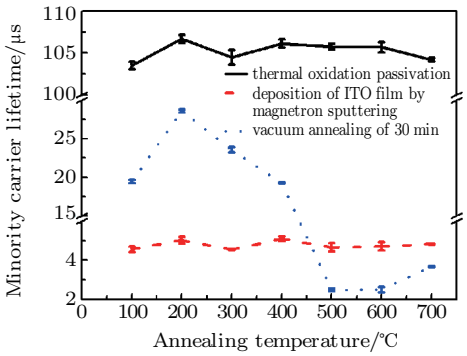


Fig. 4. (color online) The varying curves of samples' τ_{eff} with the temperature, the samples including normal thermal oxidation of silicon, then deposition of ITO film on silicon by magnetron sputtering and a vacuum annealing for 30 min, respectively ("I" represents the standard deviation).

Based on the definition and description of efficient minority carrier lifetime in Subsection 3.1, the lowering of the τ_{eff} either in the sputtering process of ITO films or in the vacuum annealing at higher temperatures must be correlated to the somehow variation of the electronic states on the surface of c-Si or inside the SiO_x or the interfacial region of SiO_x/c-Si, because the τ_{surf} is very sensitive to the changes of the chemical components on the top several layers of SiO_x/c-Si. Thus, it is necessary to extract the microstructure information within the interfacial region between ITO and c-Si so as to gain essential cause to induce the lessening after the sputtering deposition of ITO film on Si. So far, the best choice and combination for the purpose of this characterization is to apply XPS for stoichiometry and TEM for phase structure determination from the surface, down to the interface and entering the bulk to the ITO/SiO_x/Si system. In Fig. 3 we have learned the physical phase and the geometrical structure of the interfacial materials through TEM. We are sure that the ITO film and SiO_x are polycrystalline and amorphous phases, respectively. In the following sections, we will investigate the chemical configuration and electronic states of the ITO/SiO_x/Si system, especially for the SiO_x and SiO_x/Si intermediate matter.

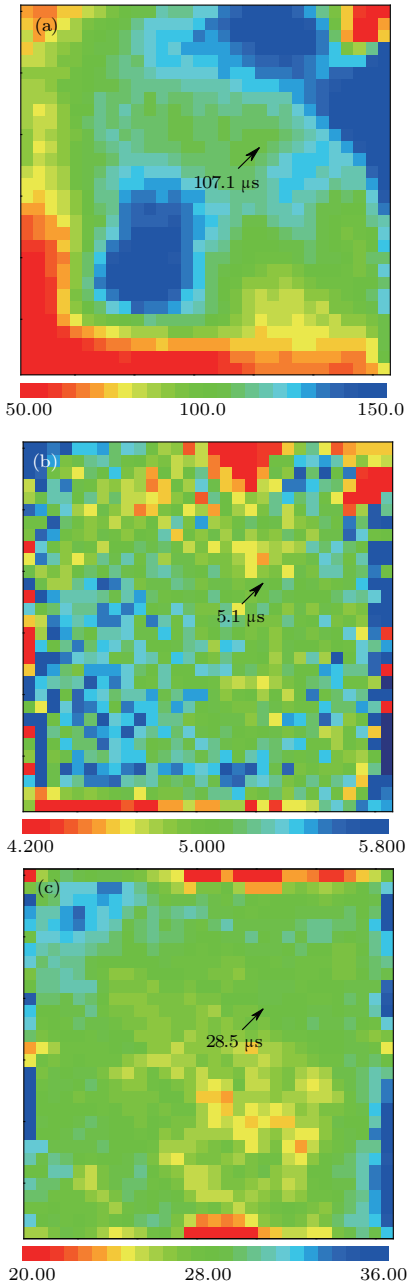


Fig. 5. (color online) Minority carrier lifetime profiles of the samples before and after 200-°C vacuum annealing, and the corresponding ITO deposition by sputtering: (a) 700-°C/10-min thermal oxide passivation; (b) ITO sputtering treatment; (c) 200-°C vacuum annealing (in unit μs).

From the point of view of the application of photovoltaic device, the last step of low temperature processing at about 200 °C is always used for the windows or electrode fabrication. The process is equivalent to the low temperature annealing treatment. Therefore, in the photoemission spectroscopy studies, we pay main attention on the annealing effect of the τ_{eff} evolution associated with the new electronic structures and chemical states of the SiO_x/c-Si for those samples after ITO deposition by sputtering method and subsequent annealing. There are two kinds of samples selected for XPS with depth profiling. One is for the annealing at 200 °C, τ_{eff} of about 30 μs. Another is for the annealing at 600 °C, τ_{eff} of about 3 μs. They are two extreme conditions for the comparison, in order to reveal the change of the fraction of S–O bonds in the intermediate region. All the Si 2p electrons emission peaks are collected at the middle position of the depth profile of chemical components as shown in Fig. 2(a), which can well manifest the variation of the electronic structures and chemical states in the SiO_x/c-Si interface.

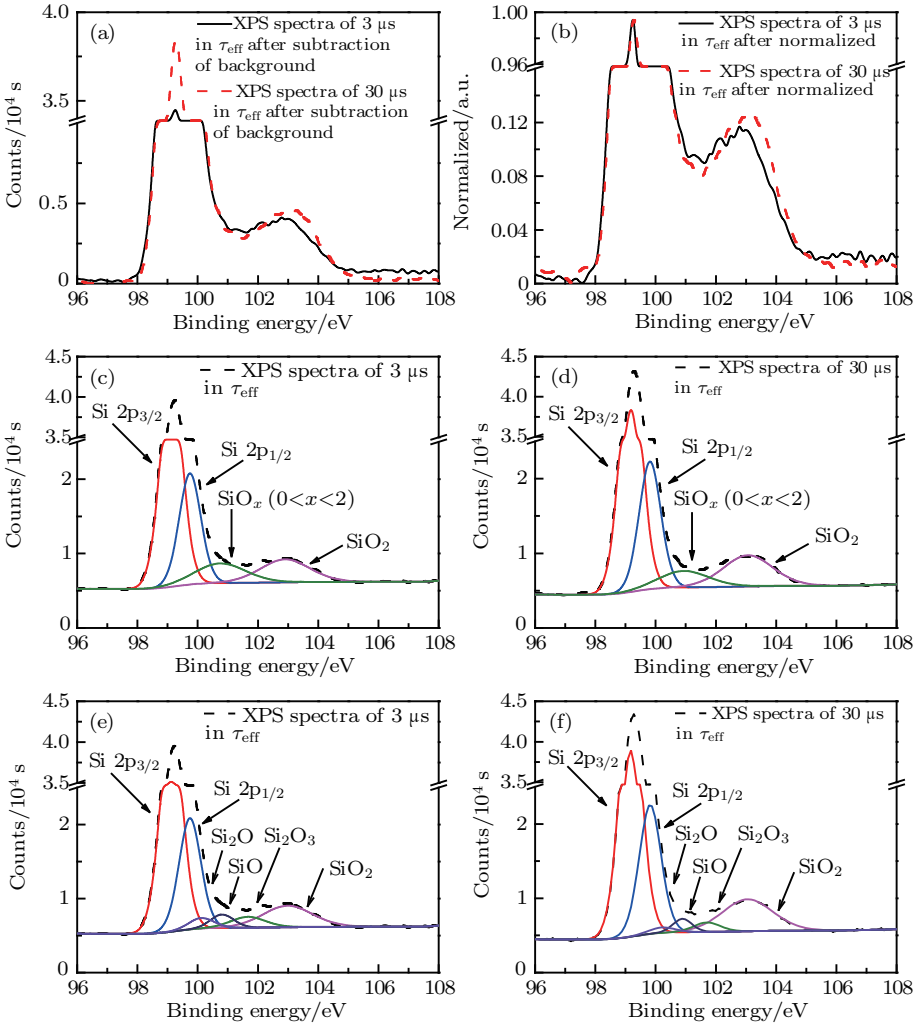


Fig. 6. (color online) Si 2p electron emission in XPS spectra for the samples at 600 °C (τ_{eff} is about 3 μs) and 200 °C (τ_{eff} is about 30 μs) vacuum annealing, respectively: (a) the subtraction of background; (b) normalized and enlarged; (c) curve fitting of Si 2p peak for 3 μs in τ_{eff}; (d) curve fitting of Si 2p peak for 30 μs in τ_{eff}; (e) secondary curve fitting of Si 2p peak for 3 μs in τ_{eff}; (f) secondary curve fitting of Si 2p peak for 30 μs in τ_{eff}.

In detail, figure 6 shows XPS spectra for the vacuum annealing samples at 600 °C (τ_{eff} is about 3 μs) and 200 °C (τ_{eff} is about 30 μs), respectively. The typical binding energies for the different Si–O bonds stoichiometric amorphous SiO_x ($0 \leq x \leq 2$) are listed in Table 1. Those XPS-Si 2p peak spectra with subtraction of the background noise in 3 and 30 μs statuses are shown in Fig. 6(a). It is apparent that there is a little difference for the peak shape of Si 2p, corresponding to SiO_x (the range of binding energy is 100 eV–102 eV) of the two samples, with this high resolution analysis ($\Delta E_{\text{Binding energy}} \approx 0.45$ eV). In addition to the illustration, a set of normalized and partially enlarged spectra, corresponding to the SiO_x component, is obviously observed in Fig. 6(b), and an intensity increase of sub-dioxide SiO_x after 600-°C vacuum annealing has been obtained. To understand these variations on the electronic structures where they are closely correlated to the SiO_x fraction in the intermediate region of ITO-Si, the deconvolution of XPS spectra for 3 and 30 μs in τ_{eff} are separately shown in Figs. 6(c) and 6(d). The Si 2p (SiO_x) peak of XPS spectra for 3 μs is stronger than that for 30 μs; oppositely,

the Si 2p (SiO_2) peak of XPS spectra for 3 μs is weaker than that for 30 μs. This contrast implies an increase of SiO_x and a decrease of SiO_2 after 600-°C vacuum annealing. Secondarily, the distinct deconvolution of XPS spectra for 3 μs and 30 μs in τ_{eff} are shown in Figs. 6(e) and 6(f), respectively. Several sub-dioxides such as Si_2O_3, SiO, and Si_2O exist in the SiO_x/c-Si interface for both samples. However, the distort Si–O bonding states in the SiO_x/c-Si interface have more of a fraction after 600-°C vacuum annealing. According to the gaseous unstable SiO forming principle proposed by Yanjun Wang *et al.*,[25] under low oxygen partial pressure (below about 10^{-4} Pa during annealing) and high temperature (500 °C–700 °C) conditions, two chemical reactions occurred in the SiO_x/c-Si interface as follows:

$$\text{Si} + \text{SiO}_2 \rightarrow 2\text{SiO}\uparrow, \tag{2}$$

$$2\text{Si} + \text{O}_2 \rightarrow 2\text{SiO}\uparrow, \tag{3}$$

where SiO (gaseous unstable substances) is difficult to be oxidized into SiO_2 phase under low oxygen partial pressure, then SiO escapes from SiO_2, which will result in an oxygen vacancy in the SiO_x/c-Si interfacial region, so that the Si dangling bonds (or interface state density) was promoted and the severe attenuation in τ_{eff} was induced.[25]

Table 1. Binding energies for amorphous SiO_x ($0 \leq x \leq 2$).[15,26] (peak error ≤ 0.10 eV).

Peak name	Peak position/eV
$Si\ 2p_{3/2}$	99.20
$Si\ 2p_{1/2}$	99.80
Si_2O	100.15
SiO	100.95
Si_2O_3	101.70
SiO_2	103.00

From the literatures, the dissociation energies of Sn–O and In–O are separately 5.47 eV and 3.59 eV in the crystallized ITO.[26] On the other hand, the unintentional oxide behavior of Si in the ITO/c-Si has been reported to grow when the sample is heat treated at high temperatures (heated at 785 °C for 33 min),[27] but the oxygen atoms (or oxygen ions) come from the decomposition of ITO materials. He *et al.* found that the sub-dioxides oxidize into SiO_2 until annealing temperature exceeds 1000 K at enough oxygen ambient.[28] However, as shown in Fig. 6(d), more SiO_2 and less SiO_x exist in the SiO_x/c-Si interface of our sample for 30 μs, indicating that additional oxygen atoms (or oxygen ions) involved in the reaction processes as Eqs. (2) and (3) under low temperature annealing (100 °C–400 °C). We did a comparison experiment to explore the source of oxygen atoms (or oxygen ions). The ITO films were directly deposited on two-faces of seven unoxidized silicon, and the samples were treated with the same processing of magnetron sputtering and post-annealing conditions. The unintentional oxide layer (seen in Fig. 3(b)) has a poor passivation effect on the Si layer (as shown in Fig. 1(e)). If these samples' τ_{eff} are not improved by low-temperature annealing, the additional oxygen atoms (or oxygen ions) are not derived from the ITO film. Figure 7 shows the varying curves of τ_{eff} with the temperature before and after vacuum annealing for 30 min (double-sided deposition of ITO by sputtering on a non-oxidized silicon wafer). The samples' τ_{eff} are unchanged before and after low temperature annealing. By comparison with low temperature parts of the annealing curve in Fig. 4, they have different trends, indicating that oxygen atoms (or oxygen ions) are derived from the SiO_x/c-Si interface rather than from the ITO film (refer to the samples with thermally grown SiO_x). Nevertheless, the vacuum annealing under 500 °C–700 °C leads to a loss in τ_{eff}. It is also verified that the occurrence of chemical reaction is like Eqs. (2) and (3). The degree of attenuation in τ_{eff} becomes weak at 700 °C, attributing to a small amount of oxygen atoms from ITO film diffused into the SiO_x/c-Si interface, which is consistent basically with the previous report.[27]

To summarize, on the one hand, the electronic structure of ultrathin silicon oxide passivation was inevitably deteriorated by energetic particles bombardment and UV light radiation during the sputtering deposition of ITO film on c-Si. Thus, the interface recombination rate of photovoltaic devices has to be increased, which is particularly prominent in the SIS and HIT devices. On the other hand, low-temperature annealing can improve samples' τ_{eff}. The following factors are implied by the above discussion: the energetic particle breaks the Si–O bond of the SiO_x/c-Si interface through impact ionization, which damages the lattice structure of the oxide layer and generates defects (Si dangling bonds). Some oxygen atoms (or oxygen ions) will obtain certain energy and diffuse to the SiO_x/c-Si interface. These oxygen atoms (or oxygen ions) will relax if their energy is less than the reaction activation energy (2 eV) of an oxygen atom in the crystalline silicon.[29] Moreover, excessive silicon ions of the SiO_x/c-Si interface have come into being in the intentional oxidation process.[16] The relaxation oxygen atoms (or oxygen ions) will react with excessive silicon ions under low-temperature annealing for 30 min, partially repairing the SiO_x/c-Si interface damage and reducing the interface states. Therefore, the passivation quality of the SiO_x layer and samples' τ_{eff} are improved. In consequence, from the formation of heterojuntion structure, establishment of built-in electric field, depositing of TCO films and preparation of external electrodes to the post-annealing process, which make it possible to prepare efficient silicon-based thin-film heterojunction solar cells in low tem-

perature and achieve a good negative temperature coefficient ($-0.25\%/^{\circ}$).[30]

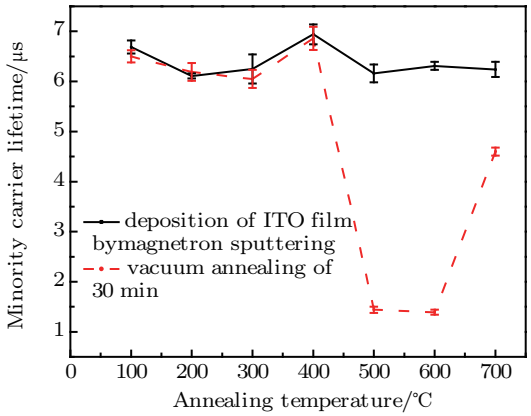


Fig. 7. (color online) The varying curves of samples' $\tau_{\rm eff}$ with the temperature before and after vacuum annealing for 30 min (double-sided deposition of ITO by sputtering on a non-oxidized silicon wafer) ("I" represents the standard deviation).

4. Conclusion

In summary, sputtering damage occurs in the process of fabricating ITO/SiO_x/c-Si photovoltaic devices, leading to a loss in $\tau_{\rm eff}$ of over 90%, decreasing to about 5 μs. Microwave photoconductivity decay experiments indicated that the sample's $\tau_{\rm bulk}$ remains unchanged before and after sputtering, and both greater than 280 μs, indicating that sputtering mainly degrades the electronic passivation quality of the SiO_x/c-Si interface. The further Si dangling bonds are created by high energy particles ($O^{+0,-1,-2}$, $Ar^{+0,+1,+2}$, $In^{+0,+3}$, $Sn^{+0,+2,+4}$) bombardment and UV radiation. These defects are verified by XPS and TEM. However, these Si dangling bonds are partially repaired under low-temperature vacuum annealing, improving the passivation effect of the SiO_x/c-Si interface. Wherein $\tau_{\rm eff}$ is restored up to nearly 30 μs at the annealing temperature of 200 °C for 30 min, which is the typical temperature in the processing of most efficient crystalline silicon heterojunction solar cells. Nevertheless, the $\tau_{\rm eff}$ can be attenuated to about 3 μs after vacuum annealing at 500 °C–700 °C for 30 min. The gaseous unstable SiO might be generated in the SiO_x/c-Si interface under this annealing condition, which damages the SiO_x/c-Si interface and increases unsaturated bonds of SiO_x, resulting in the attenuation of $\tau_{\rm eff}$. As a result, the structural sputter-induced damage is partially recovered under low-temperature vacuum annealing, which is helpful for the construction and the performance improvement of the SIS photovoltaic devices.

Acknowledgments

Financial supports were given in the footnote on the first page. Some of the measurements were conducted by the Instrumental Analysis and Research Center of Shanghai University.

Appendix A: Supplementary information

A1. The compositions of ultra-thin SiO_x layer

A thin SiO_x layer was produced by thermally oxidizing in an oxidation furnace for 10 min at 700 °C. The flow ratio of high purity nitrogen and oxygen was 4 L/min:1 L/min. The thin SiO_x layer was made up of four compositions: plenty of SiO_2, very few of Si_2O, SiO, and Si_2O_3 (as shown in Fig. S1).

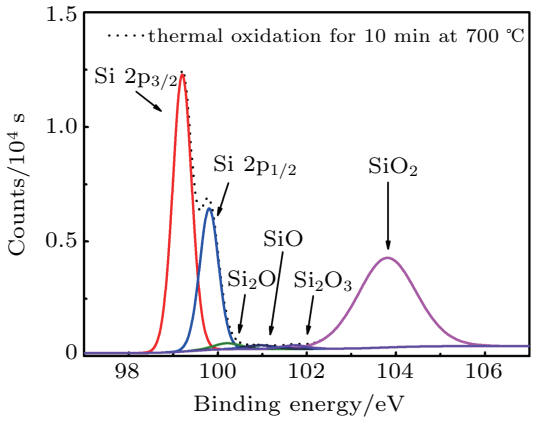


Fig. S1. (color online) The Si 2p XPS spectra of ultra-thin SiO_x layer (thermal oxidation for 10 min at 700 °C).

A2. The optical characteristics of ITO film

The optical characteristics of ITO film were measured by UV-VIS spectrophotometer. The average transmittance of the visible spectrum is more than 85% and the optical band gap was extrapolated to be 3.60 eV (as shown in Fig. S2).

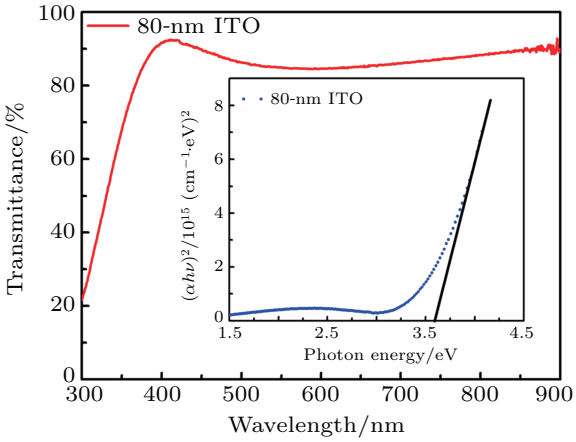


Fig. S2. (color online) The transmittance spectra of ITO film (80 nm) on glass.

References

[1] Shewchun J, Dubow J, Wilmsen C W, Singh R, Burk D and Wager J F 1979 *J. Appl. Phys.* **50** 2832
[2] Gu J H, Si J L, Wang J X, Feng Y Y, Gao X Y and Lu J X 2015 *Chin. Phys. B* **24** 117703
[3] Ashok S, Sharma P P and Fonash S J 1980 *IEEE T. Electron Dev.* **21** 725

[4] Maruyama T and Fukui K 1991 *J. Appl. Phys.* **70** 3848
[5] Chiou B S, Hsieh S T and Wu W F 1994 *Appl. Surf. Sci.* **74** 297
[6] Demaurex B, Wolf S D, Descoeudres A, Holman Z C and Ballif C 2012 *Appl. Phys. Lett.* **101** 171604
[7] Rossnagel S M 1989 *J. Vac. Sci. Technol. A* **7** 1025
[8] Mattox D M 1989 *J. Vac. Sci. Technol. A* **7** 1105
[9] Tominaga K, Chong M and Shintani Y 1994 *J. Vac. Sci. Technol. A* **12** 1435
[10] Street R, Biegelsen D and Stuke J 1979 *Philosophical Magazine Part B* **40** 451
[11] Lu M J, Bowden S, Das U and Birkmire R 2007 *Appl. Phys. Lett.* **91** 063507
[12] Zhang D, Tavakoliyaraki A, Wu Y, Swaaija R A and Zemana M 2011 *Energy Procedia* **8** 207
[13] Meng X J, Ma Z Q, Li F, Shen C, Duan Y T, Zhao L, Li Y H and Xu F 2010 *Chin. Phys. Lett.* **27** 076101
[14] Li F, Ma Z Q, Meng X J, Lu P, Yu Z S and He B 2010 *Chin. Sci. Bull.* **55** 1828
[15] Seah M P and Spencer S J 2003 *Surf. Interface Anal.* **35** 515
[16] Liu E K, Zhu B S and Luo J S 2012 *The Physics of Semiconductors* (Xi'an: Xi'an Jiao Tong University Press) p. 222 (in Chinese)
[17] Du H W, Shen L, Ding H, Yang J, Zhao L and Ma Z Q 2012 *Chin. J. Mate. Rese.* **26** 461 (in Chinese)
[18] Horfinyi S J, Pavelka T and Tutto P 1993 *Appl. Surf. Sci.* **63** 306
[19] De Wolf S, Olibet S and Ballif C 2008 *Appl. Phys. Lett.* **93** 032101
[20] De Wolf S, Ballif C and Kondo M 2012 *Phys. Rev. B* **85** 113302
[21] Du H W, Yang J, Li Y H, Xu F, Xu J and Ma Z Q 2015 *Appl. Phys. Lett.* **106** 093508
[22] Takagi Y, Sakashita Y, Toyoda H and Sugai H 2006 *Vacuum* **80** 581
[23] Luo Y R 2005 *Data Book of Bond Energy* (Beijing: Science Press) p. 279 (in Chinese)
[24] Gruenbaum P E, King R R and Swanson R M 1989 *J. Appl. Phys.* **66** 6110
[25] Wang Y J 2010 "Study of the solutions to the STI oxide AA damage defects", Master Dissertation (Shanghai: Shanghai Jiao Tong University) pp. 21–22 (in Chinese)
[26] Mitoma N, Aikawa S, Gao X, Kizu T, Shimizu M, Lin M F, Nabatame T and Tsukagoshi K 2014 *Appl. Phys. Lett.* **104** 102103
[27] Ow-Yang C W, Shigesato Y and Paine D C 2000 *J. Appl. Phys.* **88** 3717
[28] He J W, Xu X, Corneille J S and Goodman D W 1992 *Surface Science* **279** 119
[29] Kamohara S and Kamigaki Y 1991 *J. Appl. Phys.* **69** 7871
[30] Taguchi M, Yano A, Tohoda S, Matsuyama K, Nakamura Y, Nishiwaki T, Fujita K and Maruyama E 2014 *IEEE J. Photovoltaic* **4** 96